

Research papers

Innovative numerical procedure for simulating borehole heat exchangers operation and interpreting thermal response test through MODFLOW-USG code



Sara Barbieri ^a, Matteo Antelmi ^{a,*}, Sorab Panday ^{b,c}, Martina Baratto ^a, Adriana Angelotti ^d, Luca Alberti ^a

^a Civil and Environmental Engineering Department, Politecnico di Milano, P.zza L. da Vinci 32, 20133 Milano, Italia

^b GSI Environmental Inc, Herndon, VA 20170, United States

^c Biological Systems Engineering, University of Nebraska-Lincoln, Lincoln, NE 68583-0726, United States

^d Energy Department, Politecnico di Milano, via Lambruschini 4, 20156, Milano, Italia

ARTICLE INFO

This manuscript was handled by J. Simunek, Editor-in-Chief, with the assistance of Giuseppe Brunetti, Associate Editor

Keywords:

Heat transport modeling
MODFLOW-USG
Borehole Heat Exchanger
Ground-Source Heat Pump
Thermal Response Test

ABSTRACT

In recent years, among renewable energies, the geothermal resource exploitation shows a constant growth; specifically, in countries engaged in CO₂ emissions reduction and dependent on energy from abroad, the low-temperature geothermal energy (geo-exchange) for air conditioning of buildings represents a cost-effective and green solution. In closed-loop systems borehole heat exchangers (BHE) are coupled with ground-source heat pumps (GSHP) constituting the key component of the heating ventilation air-conditioning (HVAC) system. Therefore, the design of the BHE and the correct interpretation of *in situ* Thermal Response Tests (TRT) are essential to supply the building energy demand. To support the design, Modflow-USG Connected Linear Network (CLN) and Drain Return Flow (DRF) packages are adapted and improved to reproduce the operation of one or more BHE in aquifers and to analyze the TRT. The improvements are compared with a previously developed numerical model and two different analytical solutions (infinite line source and moving line source) by imposing a constant heat rate injection into the aquifer. The results show good agreement between the new approach and previous ones (discrepancy lower than 2% for models with highly refined grid), but the new approach is much more accurate and expeditious in both implementation and execution, also allowing for an easy numerical simulation of multiple BHE.

1. Introduction

EU legislation evolved significantly to achieve the EU Paris Agreement commitments for reducing greenhouse gas emissions by setting, through EC 2018/2001 Directive, the share of renewable energy by 2030 equal to 32 % of final energy consumption. As buildings are responsible for around 36 % of energy consumption and for 34 % of CO₂ emissions in Europe (European Commission, 2021), in 2016 through the “Clean Energy for all Europeans package” it was possible to target the efficiency improvement of new and existing buildings, by requiring an annual increase in the heating and cooling use of renewables of about 1.3 %.

Since Ground-Source Heat Pump (GSHP) and Groundwater Heat Pump (GWHP) systems are among the cleanest and most energy efficient

Heating Ventilation and Air-Conditioning (HVAC) systems for buildings, the exploitation of this technology has been expanding all over the world in recent years (Chae et al., 2022; Farabi-Asl et al., 2019; Jodeiri et al., 2022; Lyu et al., 2020; Sakellari and Lundqvist, 2003). According to the last pre-pandemic statistical report by GSE (Italian Energy Services Manager), in 2019 in Italy 3392 Terajoules of thermal energy were produced by exploiting GSHP or GWHP systems: although it represents only 0.15 % of the total consumed thermal energy, it increases at a yearly rate of 1.5 %.

GSHP systems are coupled to the ground by means of a closed-loop ground heat exchanger. The latter can either be composed of vertical U-shape pipes (called Borehole Heat Exchangers, BHEs), or of horizontal pipes, where a non-freezing fluid (water mixed to glycol solution) is circulated to absorb heat from the ground during the cold season and inject it during the warm one (Lyu et al., 2020). On the other hand,

* Corresponding author.

E-mail address: matteo.antelmi@polimi.it (M. Antelmi).

Nomenclature	
Symbol	Variable [unit]
α	Thermal diffusivity [m^2s^{-1}]
C_m	Volumetric heat capacity of the medium [$\text{Jm}^{-3}\text{K}^{-1}$]
c_s, c_w	Specific heat capacity of solid and water [$\text{J}/(\text{kg.K})$]
Δq	Index of accuracy for the validation process [%]
ΔT	Temperature difference between inlet and outlet fluid of the BHE [K]
D_l, D_t	Longitudinal and transversal thermal dispersion coefficient [m^2s^{-1}]
h	Convective heat coefficient [$\text{W}/(\text{m}^2\text{K})$]
i	Hydraulic gradient [-]
K_x, k_z	Hydraulic conductivity [m/s]
$\lambda_{\text{eff}}, \lambda_{\text{HDPE}}, \lambda_s, \lambda_w$	Effective thermal conductivity of medium, HDPE, solid and water [$\text{W}/(\text{m.K})$]
m	Mass flow rate [kg/s]
Q	Heat rate [W]
$q_{\text{fit}}q_{\text{num}}$	Specific heat rate, specific heat rate obtained with the interpolation process and simulated numerically [W/m]
ρ_b	Bulk density [kg/m^3]
R_b	Borehole thermal resistance [K.m/W]
r_b	Borehole inner radius [m]
S_y, S_s	Specific yield [-] and specific storage [m^{-1}]
$T_f, T_{\text{in}}, T_{\text{out}}, T_o, T_{\text{sub}}$	Circulating fluid mean temperature, Temperature of the inlet/ outlet fluid of the BHE, Temperature of the undisturbed ground and Temperature of the subsoil [°C]
t	Time [s]
v	Darcy velocity [m/s]
v_{eff}	Effective heat transport velocity [m/s]
Φ	Aquifer porosity [-]
BHE	Borehole Heat Exchanger
CLN	Connected Linear Network
COP	Coefficient Of Performance
DRT	Drain with Return Flow
GLHE	Ground Loop Heat Exchanger
GSHP	Ground Source Heat Pump
HDPE	High-Density Polyethylene
ILS	Infinite Line Source
MLS	Moving Line Source
TRT	Thermal Response Test
TSPEP	Two-Step Parameter Estimation Procedure

GWHP systems are based on injecting and extracting wells (open-loop system), similar to those generally used for Pump&Treat systems (Antelmi et al., 2020b) except that in this case water is used to produce energy. The Coefficient of Performance (COP) of these systems reaches higher values than conventional air-source heat pumps, since the ground is often cooler in summer and warmer in winter than the air temperature (Li et al., 2014).

GSHP systems performance and design is highly dependent on the heat transfer capability between the BHE and the subsoil, and thus the estimate of the thermal subsoil properties is essential (Pambou et al., 2022). The execution of the so-called Thermal Response Test (TRT) on subsoil is always recommended for a better HVAC system design and sometimes it is also mandatory: e.g., in Lombardy Region, Italy, a TRT is required (Regione Lombardia, 2010) for GSHP systems with heat rate greater than 50 kW. This test is performed to evaluate the effective thermal conductivity of the soil λ_{eff} and the borehole thermal resistance R_b (Gehlin, 2002; Spitzer and Gehlin, 2015; Zhang et al., 2014). It is carried out on a pilot BHE connected to a testing unit and is performed by supplying a constant heat rate to the circulating fluid by means of an electrical resistance (Naldi and Zanchini, 2019). Inlet and outlet fluid temperatures are recorded throughout the test along with water flow rate, electrical power related to the thermal resistance and external air temperature. (Blasi and Menichetti, 2012) stated that the standard deviation of the thermal conductivity is equal to $\pm 15\%$ when the test is conducted with a duration of about 20 h, whereas it is reduced to $\pm 5\%$ for a test lasting about 50 h. The presence of groundwater flow could complicate the assessment of the thermal conductivity, so that performing the test over 72 h is suggested; indeed, over that time, the available literature suggests that the ground response to the thermal excitation achieves a steady-state condition for all aquifers that have been studied (Antelmi et al., 2021; Beier, 2021; Nieto et al., 2020; Zhang et al., 2022).

Different approaches can be applied to the analysis of the experimental data recorded during the TRT: both simplified analytical models (Banks, 2012; Carslaw and Jaeger, 1959; Diao et al., 2004; Molina-Giraldo et al., 2011; Pasquier and Lamarche, 2022) and more complex numerical models allowing to include more elements that influence test results (Casasso et al., 2017; Casasso and Sethi, 2014; Zong et al., 2021). Due to their simple mathematical formulation and to the limited number of input parameters, the analytical models of the Infinite Line Source

(ILS) and the Moving Line Source (MLS) are the most common approaches adopted for the interpretation of TRT data (Carslaw and Jaeger, 1959; Diao et al., 2004). Both models assume the GSHP system as an infinite linear heat source exchanging heat with the homogeneous and isotropic surrounding ground with a constant heat flux per unit length (Bandos et al., 2009; Eskilson, 1987; Man et al., 2010; Zeng et al., 2002). The difference between the two models is that the ILS assumes pure conduction in the ground, whereas the MLS also considers the advection term due to groundwater flow. Therefore, the ILS model application is restricted to the geological sites where groundwater flow is absent or negligible, otherwise, a more suitable solution is the MLS (Diao et al., 2004; Sutton et al., 2003; Wagner et al., 2013). In the end, applying both the ILS and MLS, only an effective value of the thermal conductivity for the entire depth of the BHE is obtained, neglecting the variation along the vertical caused by a heterogeneous lithostratigraphy.

Numerical models represent a more complex but potentially more precise solution to evaluate the correct aquifer thermal parameters (Attard et al., 2020; Fujii et al., 2005; Giordano et al., 2021). They need more input parameters derived from a specific Conceptual Site Model (CSM), but they are flexible tools able to simulate non-ideal conditions (e.g., heterogeneous soils, realistic surface boundary conditions, geothermal gradients etc.) and relevant physical processes (namely, beside conduction, advection and thermal dispersion). These tools coupled with suitable parameter estimation procedures provide more accurate results (Antelmi et al., 2020a; Dalla Santa et al., 2022; Galgaro et al., 2021). When reproducing a BHE in a numerical model, the main components involved are characterized by different dimensions: from millimetres (pipe thickness) to meters (aquifer) (Angelotti et al., 2014a). When a fully 3-D approach is applied, the multiple spatial scales lead to numerical models affected by high computational loads. (Angelotti et al., 2014b) developed a 3-D numerical finite-difference model by means of MODFLOW code coupled to MT3DMS of a single BHE by turning its circular section to an equivalent square one. Although the numerical model was validated for different groundwater flow velocities, its applicability was limited due to the large number of model domain cells that did not allow to represent more than one BHE. (Marcotte and Pasquier, 2008), simulating the thermal behaviour of a vertical BHE, implemented a 3-D finite element numerical model through the COMSOL code; by exploiting the symmetry of the problem they were able to halve the number of cells and partially reduce the

computational burden.

The reduction of the cells number for aquifer and BHE representation was also achieved using a 1-D (Shonher and Beck, 1999) and a 2-D numerical modelling approach (Berberich et al., 1994; Wagner and Clauser, 2005) or alternatively, by applying a reduced-order numerical approach that couples a 1-D description of the vertical pipes heat transfer with a 3-D description of the aquifer (Signorelli et al., 2007). The latter created a finite-element model of a BHE system in the fractured geological formation, which is suitable to simulate coupled hydraulic and thermal processes under non-steady conditions. The authors used synthetic TRT data from the numerical model to evaluate the sensitivity of the ILS model analysis to test duration, borehole length, groundwater velocity and subsurface heterogeneity. The model implemented 3-D elements reproducing the porous matrix around the BHE and 1-D pipe elements for the BHE implementation; the heat transfer between the circulating fluid and the aquifer was simulated as a thermal resistance related to the velocity-dependent heat transfer coefficient of the fluid. A similar method is used also in (Lamarche et al., 2010) to compare different empirical and theoretical approaches for the evaluation of the borehole resistance. The authors implemented a 3-D numerical model in COMSOL reproducing the borehole by means of 1-D finite elements using the traditional advective equation. Another study developed in COMSOL is the one by (Bozzoli et al., 2011), where a Two-Step Parameter Estimation Procedure (TSPEP) for the evaluation of the grout and soil thermal conductivities is validated using both simulated and experimental data. As for the previous studies, heat transport in the BHE was simulated through 1-D equations, while heat transfer in the hydrogeological domain through 3-D equations. (Brunetti et al., 2017; Šimánek et al., 2016) adopted the coupling of a 2-D domain to implement the aquifer and a 1-D domain for the BHE in the HYDRUS code. The two domains were connected by a Robin boundary condition which enabled the simulation of heat transfer between the BHE and the surrounding soil. The proposed numerical TRT was validated against experimental data collected in two sites in Japan. Similar studies about pseudo-3-D models for the simulation of GSHP operation are reported in (Al-Khoury et al., 2005; Florides et al., 2012; Raymond et al., 2011).

The aim of the present study is to provide an updated, simple, improved and expeditious numerical tool to analyse in situ TRT through MODFLOW, specifically the version MODFLOW-USG, a widely used code for modelling environmental problems in groundwater. The novelty of the updated tool is the introduction into the CLN package of new characteristic elements of a BHE, such as the thickness and the thermal conductivity of the U-pipe and the internal convective heat transfer coefficient. Another important improvement is the option to couple the Connected Linear Network (CLN) and Drain Return Flow (DRT) packages, to simulate the heat carrier fluid circulating in the BHE and injecting a constant heat rate into the ground. This allows to simulate a TRT and to validate the CLN approach comparing it with the available constant heat rate analytical solutions. These enhancements are key to reproduce each thermal resistance between the circulating fluid and the aquifer, thus accurately reproducing the heat transfer nearby the BHE through a 1-D approach for the fluid. Therefore, besides providing an effective method to simulate and analyse a TRT, the proposed tool, without the DRT Package, can be used to expeditiously simulate the typical operation (heating/cooling) of a GSHP system consisting of multiple BHE avoiding numerical convergence problems. In the present paper different numerical models at constant heat rate injection are developed, featuring four spatial discretizations, and a sensitivity analysis on groundwater velocity is performed. Each model is then tested against common analytical models (ILS and MLS) and compared with the numerical models discussed in (Angelotti et al., 2014a).

2. Material and methods

A synthetic numerical model of a single BHE with hydrogeological and thermal properties adapted from (Angelotti et al., 2014a), is

implemented in MODFLOW-USG by applying the approach tested in (Antelmi et al., 2021). The graphical user interface is Groundwater Vista 7.0 (ESI, Inc.). The CLN package has been updated in some programming features compared to the version package discussed in (Antelmi et al., 2021); whereas, the DRT package is specifically adapted to create a constant heat rate injection in aquifer, such as in TRT execution. A complete description of the package modification is presented in the next pages.

2.1. MODFLOW-USG and CLN

MODFLOW-USG (Panday et al., 2013) is an open access numerical code for modeling groundwater flow. The main advantage over previous versions of MODFLOW is the Control Volume Finite Difference (CVFD) approach, which is a generalization of the finite-difference approach that allows the use of unstructured grids. The other characteristic that distinguishes MODFLOW-USG is the solution of tightly coupled processes that interact with groundwater flow; thus, every equation of the model is solved in one matrix, avoiding convergence problems. Specifically, the CLN package simulates one-dimensional features such as pipes, wells, karst conduits, or streams that interact with groundwater flow. Since its release, MODFLOW-USG has been expanded to include solute and heat transport; such features are available as open access software USG-Transport (Panday, 2020). The Heat Transport Package is well suited for simulating geothermal plants impacts and CLN Package is well suited to simulate a BHE, as it was demonstrated by (Antelmi et al., 2021).

In previous works, the numerical modeling of BHE with MODFLOW/MT3DMS was faced for the first time by (Angelotti et al., 2014a). That paper aimed to prove the capability of these codes to model BHEs with a good accuracy and to fully discuss the influence of groundwater flow on the energy performance of BHEs and on the aquifer temperature distribution. The U-pipe geometry, the thermal-carrier fluid flow and aquifer temperature distribution were explicitly reproduced for the first time, going beyond previous applications of numerical codes. The main challenge was to correctly reproduce the BHE in a homogeneous aquifer through a square or rectangular grid (classic Finite Difference grid of MODFLOW-2000). To this purpose, the U-shape pipe was represented by a square section requiring a very fine horizontal and vertical discretization (minimum cell size 0.37 cm). The pipe size was derived on the assumption of conserving the total thermal resistance per unit length between circular section and square one. In specific, the total thermal resistance was calculated as the sum of a convective resistance and of a conductive one.

An extensive validation of the numerical model solutions was provided comparing them with the analytical MLS solution, assimilating the U-pipe to an infinite line source and varying the groundwater velocity. The heat exchange rate was not imposed as a boundary condition but resulted from the interaction between the BHE and the surrounding porous medium. The simulation results provided an evaluation of the temperature perturbation in the aquifer, improving the energy exchange estimation and providing a quantitative assessment of the heat rate increase due to groundwater flow.

CLN elements can be vertical, horizontal, or inclined and can have rectangular or circular shaped cross-sectional geometries. Their connection for flow and transport to groundwater flow (GWF) cells occurs through analytic equations that include skin/efficiency factor considerations. MODFLOW-USG accommodates vertical, horizontal, or angled CLN elements. Groundwater Vista allows for input of CLN as a "CLN well" or a "CLN polyline": the former is vertical and used to represent vertical conduits (e.g., a well), while CLN polylines can be implemented at any angle (e.g., hydraulic pipes). In the current implementation, the CLN polyline is used to connect 2 vertical CLN wells to reproduce the real geometry (U-shape pipe) of the BHE (Fig. 1).

Additional enhancements have been applied to the BHE simulation process since the discussions in (Antelmi et al., 2021). Specifically, three

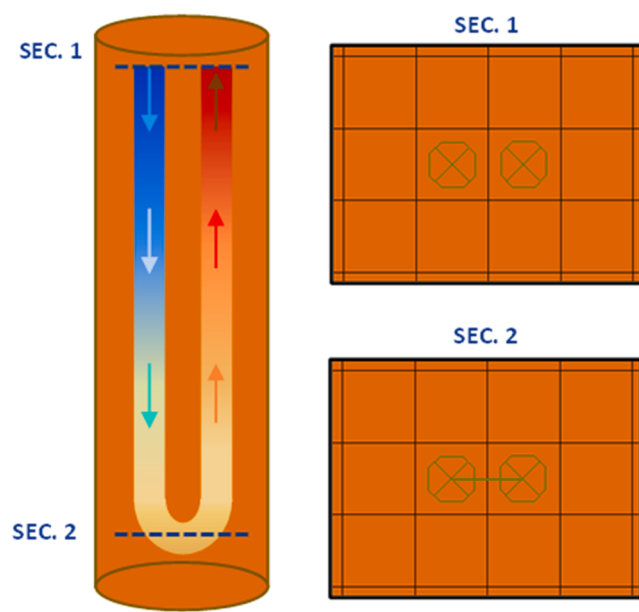


Fig. 1. BHE sections and geometry representation through CLN. Rectangles are groundwater cells, octagons are CLN Wells and the line connecting the bottom octagons is the CLN polyline.

characteristic parameters of the BHE are introduced in the numerical code:

According to $H=mst$ formula

- the U-pipe (i.e. high density polyethylene) thickness;
- the U-pipe thermal conductivity;
- the internal convective heat transfer coefficient.²¹

When the aim of the numerical simulation is to describe what happens into the BHE and the cells strictly surrounding it, these parameters need to be considered. The enhancement improves the accuracy of the numerical representation of the BHE and the heat transport between groundwater and BHE. The net thermal resistance between aquifer and BHE is a sum of 2 resistances: the conductive resistance offered by the BHE pipe wall and the convective one, related to the BHE circulating fluid. The latter is depending on the convective heat transfer coefficient, that is linked to the inner diameter of the BHE tube, to the fluid flow rate and regime (laminar or turbulent).

Another enhancement to the MODFLOW-USG software specific for the implementation of BHEs and the simulation of a TRT was to provide appropriate boundary conditions to the inlet and outlet of the BHE tube as discussed below.

2.2. Boundary conditions for the BHE

MODFLOW-USG includes several packages to provide boundary conditions to a simulation. These boundary conditions can be applied to the GWF and/or the CLN domains. For instance, a flow rate and a temperature may be provided at the inlet of the BHE tube and the code will compute the flow rate and temperature at the outlet.

For a BHE, the outflow rate will be equal to the inflow rate, which may be applied as an outflow boundary condition. If the flow in the BHE tube is at steady-state conditions, a reference head is required for a unique solution to the flow in the BHE tube. Thus, a prescribed source flux may be provided at the inflow end. At the outflow end, a reference head may be provided to allow the BHE fluid to exit (it can be any value above the top of the model domain such that the tube remains fully saturated at the outlet point).

Typical operation of a TRT requires a constant heat rate injection. Thus, the temperature at the outlet of the BHE is at a constant

differential from the temperature at the inlet. The DRT package²² available in MODFLOW-USG-Transport was modified to accommodate this condition. This package was developed to extract water from cells characterized as a drain and re-inject all or part of it into another cell. This feature was expanded for use with solute and heat transport problems: it allows to link the solute concentration, or temperature, extracted from the drain cell (which can be the CLN cell representing the borehole outlet), with that of re-injected water (into the CLN cell representing the borehole inlet).

By using the BHE outlet as a drain cell and the BHE inlet as a re-injection cell, it is possible to create a closed loop circuit as in a TRT or in the common operation of a BHE. Since a reference head is required in the BHE for a steady-state solution, an option is provided which allows for extraction of water under a Cauchy boundary condition²³, which provides the reference head. In the DRT package file, the reference head and the return flow rate are then set by the user and supplied to the BHE outlet and inlet CLN nodes, respectively, to provide the appropriate flow within the BHE tube. This case is called the GHB-Q condition²⁴ and is identified by providing a negative conductance factor in the DRT package input file (Panday et al., 2013). The value is converted to positive internally in the code.

A temperature difference (ΔT) can then be forced between the outflow and inflow such that the system operates under a constant heat rate. The heating power actually depends on the mass flow rate of the heat transfer fluid, on its heat capacity per unit mass and on the temperature difference ΔT . Since the mass flow rate and the heat capacity are constant over time, ΔT is the only quantity that must be forced to remain constant during the simulation. This requirement can be satisfied within the DRT input file, where a fixed temperature increase can be added to the drained temperature before reapplying the water flow rate at the return-flow location. This procedure allows an automatic implementation of the ΔT , thus overcoming the method adopted so far with MODFLOW/MT3DMS, which required the simulation to be interrupted many times to manually adjust this parameter.

Therefore, to properly use the DRT package, the following information must be introduced into the input data file: the node number of the inlet and outlet cell of the BHE, the elevation of the water level for the GHB-Q condition, the flux rate applied to the return flow node and the fixed temperature increase at the BHE inlet node.

2.3. Numerical model implementation

Three main features are essential to numerically reproduce a conventional TRT:

- the real pipe circular section of the BHE;
- the circulation of the fluid inside the BHE;
- a constant heat rate injection into the ground during the test.

When the numerical code involves only rectangular or square cells, such as MODFLOW and MT3DMS, the circular geometry of the BHE must be approximated through an equivalence with a square or rectangular one. Angelotti et al. used this approach with good results (Angelotti et al., 2014a), although with a big effort in terms of computational load and implementation times: running the numerical model for one specific groundwater flow velocity required more than 1 day for an expert user and a significant effort to find the right combination of numerical solver parameters to achieve convergence. In specific, each square section of the BHE pipe consisted of 36 cells, reproducing the heat carrier fluid, surrounded by 0.37 cm cells representing the HDPE; the U-shaped elbow was implemented through two outer horizontal layers with a thickness of 0.37 cm and one in the center of 3.36 cm.

Differently, in the present study the BHE is implemented in accordance with the approach proposed and validated by (Antelmi et al., 2021) by means of three analytical elements: two CLN Wells representing the inlet and outlet pipes and one horizontal CLN Polyline

implementing the elbow of the U-tube. Since all these elements are circular, this approach better reproduces the real geometry of the system, while the unstructured grid approach allows to use a coarse grid (more details in subsection 2.4). Furthermore, as already mentioned in subsection 2.1, the new version of CLN package, specifically updated for this study, allows the user to include the HDPE thickness, although CLN elements are 1D, together with the HDPE thermal conductivity and the convective heat transfer coefficient. The solver used for the numerical simulations is the Sparse Matrix Solver (SMS)²⁵, which includes a Total Variation Diminishing (TVD) scheme²⁶ to control numerical dispersion²⁷ in the advection term. An adaptive time-stepping solution²⁸ was selected, automatically adapting the time step length to satisfy the Courant number constraints. The computational time of each simulation²⁹ is lower than 1 min for any groundwater flow velocity (Intel(R) Core (TM) i9-9900K CPU @ 3.60 GHz).

In (Angelotti et al., 2014a), the authors simulated the constant heat rate operation of the BHE, maintaining the heat carrier fluid circulation by means of Constant Head (CH) condition at the inlet and outlet of the U-pipe and subdividing the total duration of the TRT into multiple simulations. During each simulation the inlet fluid temperature was defined as a function of the outlet fluid temperature at the last time step of the previous simulation using the equation:

$$T_{in} = T_{out_{n-1}} + \frac{Q}{mc_w} \quad (1)$$

where Q [W] is the constant heat rate injected into the ground, m [kg/s] is the mass flow rate into the BHE and c_w [J/(kg K)] is the specific heat capacity of the heat carrier fluid.

This manual methodology caused a high computational load and a significant loss of time to adapt each simulation. Differently, the new procedure here discussed leads to a rapid “automatic approach” using the DRT package for both circulating the heat carrier fluid and maintaining a constant heat rate injection during the test. The user needs to specify the flow rate circulating in the pipe (Table 1), the inlet and the outlet U-tube nodes where water is injected and extracted and the temperature difference to add to the fluid before its re-injection in order to maintain a constant heat rate of 40 W/m.

The case study implemented in MODFLOW-USG corresponds to the synthetic model discussed in (Angelotti et al., 2014a). It includes a BHE in a homogeneous saturated sandy and non-dispersive aquifer³⁰. The BHE features are provided in Table 1. The presence of the borehole filling material does not significantly influence neither the energy exchange nor the temperature profile into the aquifer (Alberti et al., 2017, 2016), therefore, the thermal properties of the grout material are assumed equal to the surrounding soil in both models. The dimensions of the modeling domain are equal to (Angelotti et al., 2014a), whereas the grid discretization is different: the quadtree refinement³¹ is used (Fig. 2) to refine the cells only in the proximity of the BHE as already applied in (Antelmi et al., 2021).

The groundwater flow direction is set through a Constant Head condition applied to the right and left boundaries cells and it results in West to East. The same boundary condition is assigned to set a constant unperturbed temperature equal to 11.8 °C, corresponding to the unperturbed temperature used in (Angelotti et al., 2014a). The thermal dispersion term is set equal to zero since dispersion is generally neglected for the heat transport in aquifer³² and is not even implemented

into analytical solutions. Hydrological and thermal properties of the model, from (Angelotti et al., 2014a), are listed in Table 2.

2.4. Grid sensitivity analysis for different Darcy velocities

The added value of this research depends not only on the innovations to the DRT and CLN packages in MODFLOW-USG, but also crucially on the different grid refinements tested to achieve the best solution under different velocity regimes. A total of 16 different models are implemented combining 4 minimum cell size values and 4 Darcy velocities. Numerical model's nomenclature and characteristics are listed in Table 3.

The horizontal grid is characterized by a local refinement around the BHE implemented through a Quadtree approach, with a minimum cell size inside the refinement box ranging from 0.5 cm (Fig. 3a) to 50 cm (Fig. 3d) and a maximum one outside the box ranging between 32 cm (Fig. 3a) and 100 cm (Fig. 3c, d). Quadtree refinement is a straightforward way to focus resolution in areas of interest implementing a finer grid with different levels of detail (Panday et al., 2013). The user can specify a maximum number of seven concentric zones where the starting grid of the model is refined with a degree of detail increasing with the number of the zones (Antelmi et al., 2021). The two CLN Wells are implemented in two different adjacent cells to avoid numerical issues and as they do not need to be placed at the grid nodes but can be placed at any coordinate, it is possible to maintain a pipe-to-pipe centers distance of 6 cm for any grid geometry.

Each model consists of 20 layers with a thickness of 9 or 10 m for a total thickness of 200 m. Clearly, the model thickness was set greater than the BHE length (100 m) to avoid any influence of the bottom boundary condition which is a no flow and no energy exchange type. The first layer and the one containing the CLN Polyline (the tube elbow) thickness is about 1 m. The refinement in correspondence of these two layers proved to be fundamental to apply the 40 W/m required thermal power. The applied groundwater flow velocities values vary from 0 to 10^{-5} m/s, to reproduce the typical range of velocities in hydrogeological natural systems.

The TRT usually lasts no more than 72 h, but here longer durations are simulated (up to 60 days). This is consistent with the study performed by (Angelotti et al., 2014a), where the duration was chosen to achieve steady state conditions in the aquifer temperature field.

2.5. Numerical model validation

(Brunetti et al., 2017; Brunetti et al., 2017) The numerical model is validated by comparison with analytical results obtained from ILS and MLS approaches, as done in (Angelotti et al., 2014a).

To verify the accuracy and validate the 16 numerical TRT simulated in MODFLOW-USG, a comparison between the two approaches was conducted in terms of aquifer temperature values downstream of the BHE. Temperature values are recorded at different time steps implementing 11 observation wells distributed at distances ranging from 0.2 m to 5.8 m from BHE-center (Fig. 4).

Each monitoring well has a depth that reaches to the elbow of the heat exchanger; according to the choice of (Angelotti et al., 2014a) temperatures refer to a representative depth of 35 m.

The validation process aims to evaluate the divergence between numerical and analytical results in energy terms, through 4 steps:

1. evaluation through the numerical model of the aquifer temperature values in correspondence of 11 monitoring wells (Fig. 4) at different time steps: $T_{sub\ num}(x_i, y = 0, t_k)$;
2. evaluation through the analytical models ILS/MLS of the aquifer temperature values downstream of the BHE: $T_{sub\ an}(x_i, y = 0, t_k)$;
3. computation of the deviation between numerical and analytical solution in terms of Root Mean Squared Error (RMSE) at every time step;

Table 1
Geometric and operational properties of the BHE.

Property	Value	Measurement Unit
Flow rate	0.277	l/s
Depth	100	m
Inner radius	0.02	m
Pipe-to-pipe centers distance	0.06	m
HDPE thickness	0.0037	m

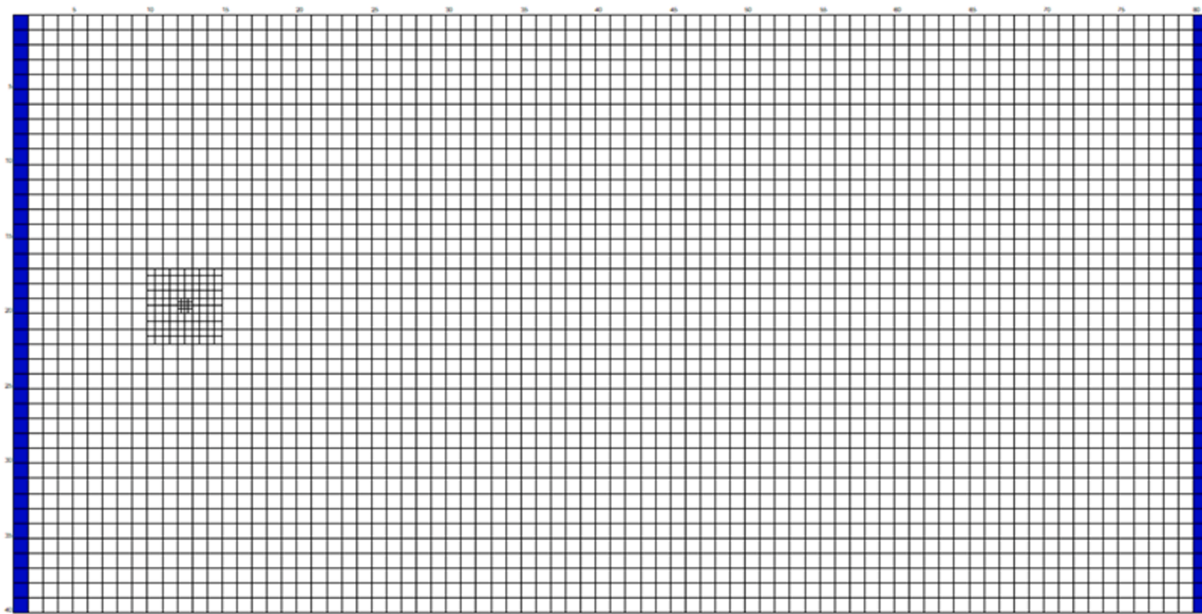


Fig. 2. Example of planar view of the numerical model domain; Constant Head condition is shown by blue cells. (For interpretation of the references to colour in this figure legend, the reader is referred to the web version of this article.)

Table 2
Hydrogeological and thermal properties implemented in the model in MOD-FLOW-USG.

Parameter	Value	Measurement Unit
Hydraulic gradient, i	$4.97 \cdot 10^{-3}$	–
Aquifer horizontal hydraulic conductivity, K_x	$2 \cdot 10^{-5} - 2 \cdot 10^{-3}$	m/s
Aquifer vertical hydraulic conductivity, K_z	$2 \cdot 10^{-6} - 2 \cdot 10^{-4}$	m/s
Groundwater Darcy velocity, v	$0, 10^{-7}, 10^{-6}, 10^{-5}$	m/s
Aquifer porosity, Φ	0.35	–
Aquifer Specific Storage, S_s	0.01	m^{-1}
Bulk density, ρ_b	1700	kg/m^3
Solid specific heat capacity, c_s	747	$J/(kg \cdot K)$
Water specific heat capacity, c_w	4154.2	$J/(kg \cdot K)$
Solid heat conductivity, λ_s	3.18	$W/(m \cdot K)$
Water heat conductivity, λ_w	0.59	$W/(m \cdot K)$
HDPE heat conductivity, λ_{HDPE}	0.38	$W/(m \cdot K)$
Convective heat coefficient, h	1137.39	$W/(m^2 \cdot K)$
BHE mass flow rate, m	0.277	kg/s
Constant design heat rate	40	W/m
Longitudinal, Vertical, Transversal Dispersivity	0	m

Table 3
Numerical models implemented.

Min cell size [cm]	V _{Darcy} [m/s]				
		0	10^{-7}	10^{-6}	10^{-5}
0.5	CLN_0.5-0	CLN_0.5-7	CLN_0.5-6	CLN_0.5-5	
6	CLN_6-0	CLN_6-7	CLN_6-6	CLN_6-5	
25	CLN_25-0	CLN_25-7	CLN_25-6	CLN_25-5	
50	CLN_50-0	CLN_50-7	CLN_50-6	CLN_50-5	
0.37	MA	MA	MA	MA	

4. minimization of the RMSE through the *fminsearch* Matlab function, using the specific heat rate in the ILS/MLS model as the minimization parameter. The achieved thermal power per unit length, named q_{fit} , along with the one simulated numerically q_{num} , allows to calculate an index of accuracy Δq of the numerical model, as in (Angelotti

et al., 2014a). To evaluate the efficiency of the heat exchange of the new approach, thus further supporting the use of this tool for the typical operation of a BHE, the same index is here calculated as:

$$\Delta q = \frac{q_{fit} - q_{num}}{q_{num}} * 100 \quad (2)$$

For a complete view of the new suggested approach, the results are also discussed in terms of heat carrier fluid mean temperature and aquifer temperature, highlighting their dependence on the horizontal discretization and on the groundwater flow velocity implemented.

Extracting the temperature at the BHE inlet and outlet nodes and computing the arithmetic mean for each time step, the mean fluid temperature T_f is calculated as:

$$T_f(t_k) = \frac{T_{in}(t_k) + T_{out}(t_k)}{2} \quad (3)$$

Finally, the results of the validation process are shown and compared with those achieved in (Angelotti et al., 2014a) through the “MA” models (Table 3).

3. Results and discussion

3.1. Heat carrier fluid mean temperature: grid sensitivity analysis for different Darcy velocities

The simulations were run under transient regime with different durations according to the different groundwater flow, as explained in subsection 2.4. From the results, an estimate of the heat carrier fluid temperature along the BHE depth, of the aquifer temperature downstream of the BHE and of the temperature variations during test time, were obtained.

The exchanged energy between BHE and aquifer was maintained constant and equal to 4000 W, by the regulation of inlet and outlet cells at the first layer of the U-shape pipe. The heat carrier fluid temperature analysis along the BHE depth is essential to understand how the energy exchange between BHE and ground layers varies along the vertical.

In Fig. 5, the trend of the heat carrier fluid temperature (T_f) as a function of time is shown for Darcy velocity equal to 10^{-5} m/s (a), 10^{-6} m/s (b), 10^{-7} m/s (c) and null (d). Due to the change in horizontal grid discretization around the BHE, for a given groundwater flow velocity (e).

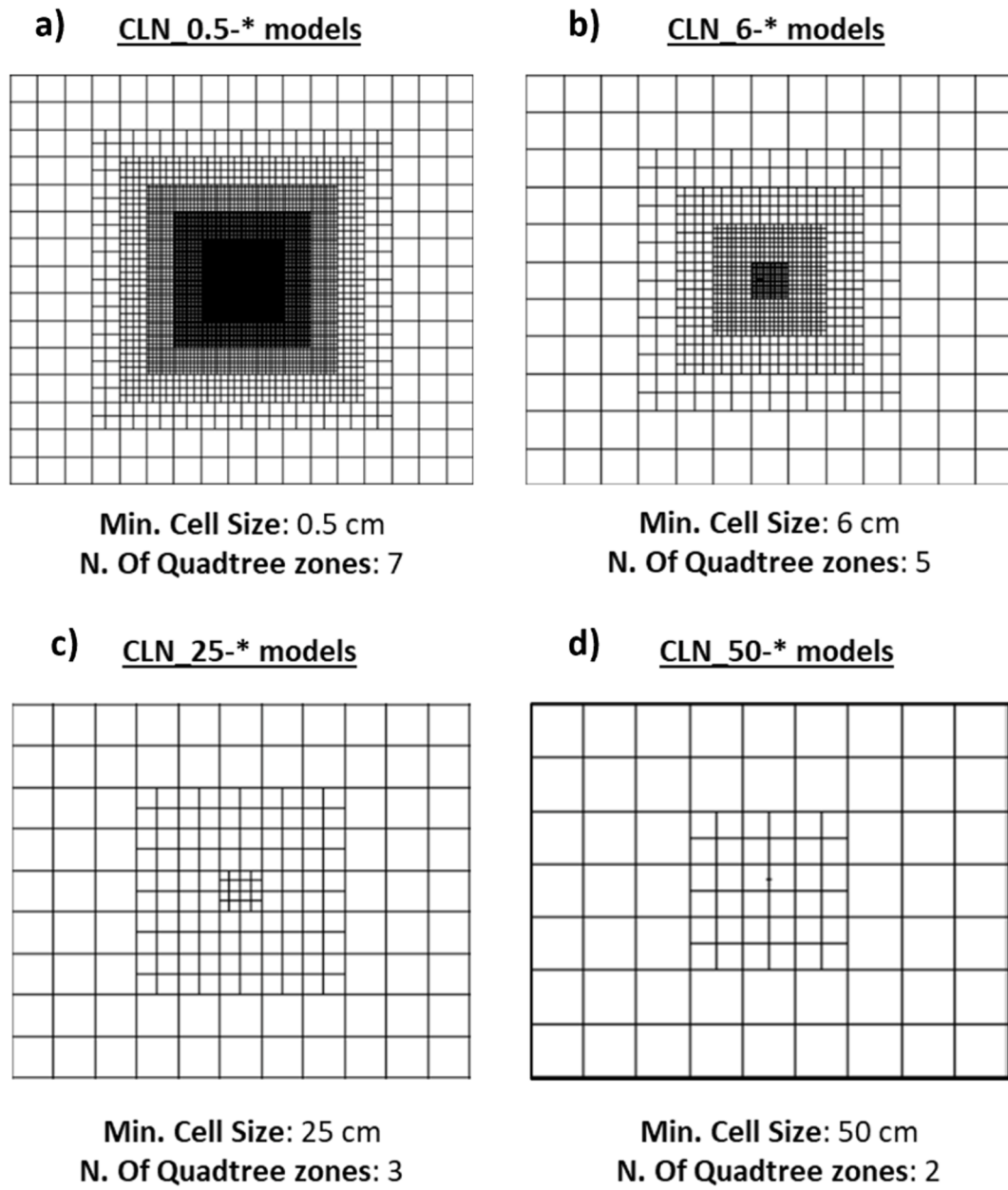


Fig. 3. Detail of the plan view of the grid refinement implemented in the numerical models.

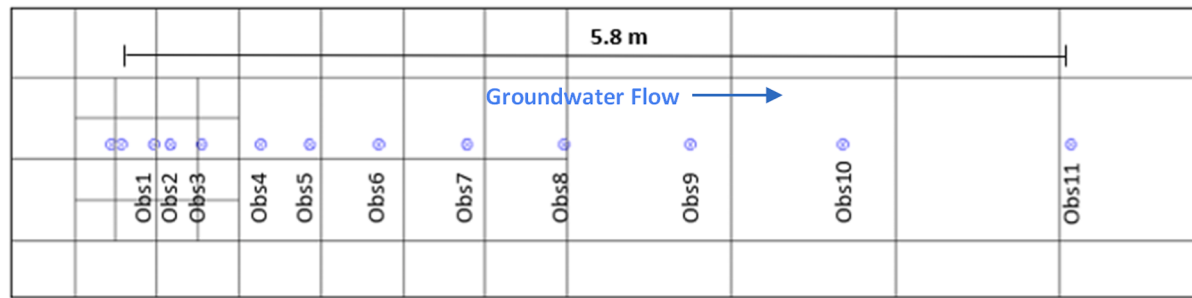


Fig. 4. Detail of the modelling domain in one of the CLN_* models, containing the 11 monitoring wells.

g. 10^{-7} m/s, Fig. 5c), lower fluid temperatures are found as the minimum cell size increases. Considering the models "CLN_*-5" (Fig. 5a), related to Darcy velocity equal to 10^{-5} m/s, at the end of the simulation, T_f

assumes values equal to 20.4, 17.8, 15.9 and 15.7 °C respectively for minimum cell size equal to 0.5, 6, 25 and 50 cm. On the other hand, as a result of the change in the plume shape around the BHE, for a given

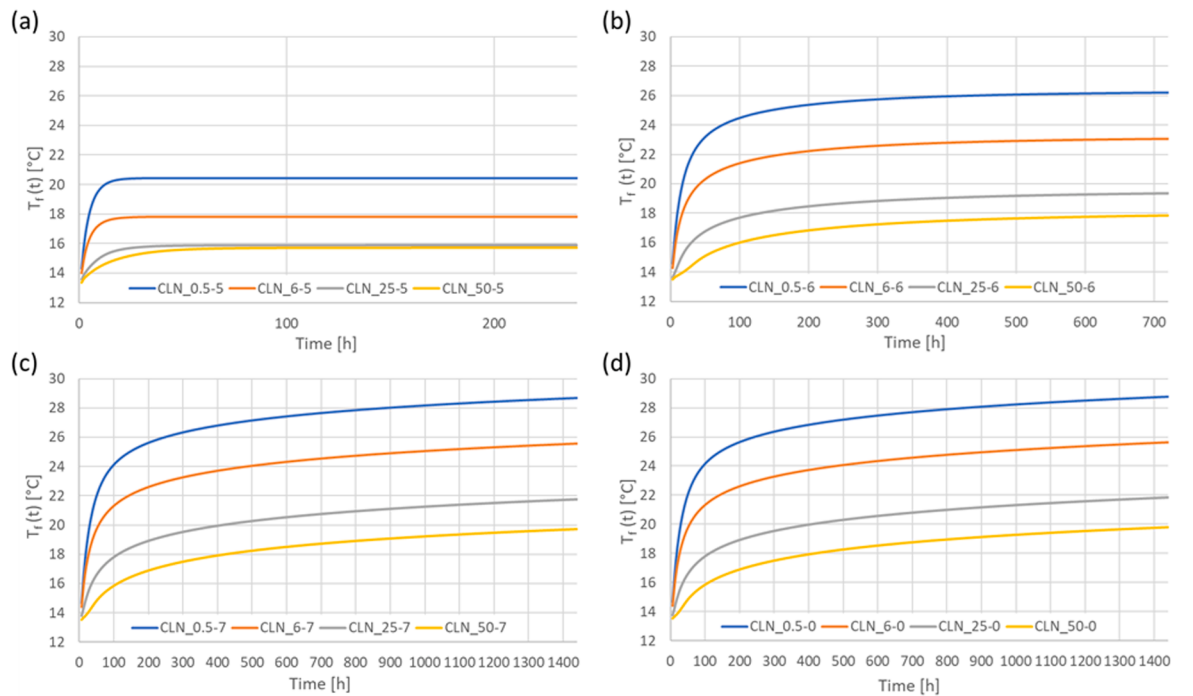


Fig. 5. Heat carrier fluid mean temperature over time simulated with “CLN _*-5” (a), “CLN _*-6” (b), “CLN _*-7” (c) and “CLN _*-0” (d) models. For each groundwater velocity the impact of the numerical grid is shown.

minimum cell size (e.g. 0.5 cm) fluid temperatures increase as the Darcy velocity decreases. Clearly, the dependence of the mean fluid temperature on the grid refinement is non-physical, while the dependence on the Darcy velocity is physically based.

Table 4 shows the main results (heat carrier fluid mean temperature T_f , difference between inlet and outlet fluid temperature ΔT from BHE, specific heat rate q_{num} and variation from the design value of 40 W/m) at the last time step of each simulation.

Despite the strong dependence of the heat carrier fluid temperatures on the horizontal discretization, the average heat rate per unit length q_{num} exchanged during the entire simulation differs by a few percentage points from the one imposed by the DRT package. A maximum deviation of -3.8% is obtained for the “CLN_50-5” model related to the greatest minimum cell size equal to 50 cm and to the maximum Darcy velocity.

The heat carrier fluid temperature distribution along the vertical, at

Table 4
Results obtained with the numerical simulations at the last time step in terms of heat carrier fluid mean temperature and simulated heat rate.

Groundwater velocity [m/s]	Min cell size [cm]	T_f at final time step [°C]	ΔT at final time step [°C]	q_{num} [W/m]	Variation from design q [%]
10^{-5}	0.5	20.42	3.44	39.41	-1.46
	6	17.79	3.42	39.30	-1.73
	25	15.91	3.39	38.99	-2.51
	50	15.72	3.34	38.47	-3.80
10^{-6}	0.5	26.22	3.45	39.16	-2.08
	6	23.06	3.43	39.19	-2.01
	25	19.35	3.43	39.32	-1.69
	50	17.82	3.42	39.33	-1.67
10^{-7}	0.5	28.71	3.44	39.05	-2.36
	6	25.58	3.43	39.09	-2.25
	25	21.74	3.43	39.27	-1.80
	50	19.71	3.43	39.35	-1.61
0	0.5	28.76	3.44	39.05	-2.37
	6	25.65	3.43	39.09	-2.25
	25	21.86	3.43	39.28	-1.79
	50	19.78	3.43	39.36	-1.58

the last time step for each numerical model (depending on flow velocity), is observed in Fig. 6.

The graphs display the temperatures of the delivery pipe on the decreasing branch of the curve (right side) and the ones of the return pipe on the increasing one (left side). As expected, the analysis confirms the behaviors described above: models with finer grids are characterized by higher temperatures (i.e. “CLN_0.5-” and “CLN_6-”); when a higher groundwater flow is implemented, at the same spatial discretization, temperatures are lower (i.e. “CLN _*-5” and “CLN _*-6”). The correct behavior of heat carrier fluid temperature as a function of depth should exhibit a decrease both during the descent and the ascent phases for any groundwater flow velocities. The Fig. 6 shows that the models with groundwater flow velocity equal to 0 m/s and 10^{-7} m/s, for each grid discretization implemented, simulate the correct temperature distribution in the BHE. On the contrary, models with Darcy velocity equal to 10^{-5} and 10^{-6} m/s simulate heat transport less accurately for 25 and 50 cm size cases. In detail, temperature values along the return pipe stop decreasing as they proceed towards the ground level, assuming, in some cases, a constant temperature value (“CLN_25-6” and “CLN_50-6”) or, in other cases, a progressively slightly increasing value (“CLN_25-5” and “CLN_50-5”). An explanation to this behavior can be achieved looking at the grid spacing. The heat exchange in the CLN domain is affected by temperatures calculated in GWF cells (outside the CLN cells area) located around the BHE; therefore, the implementation of different horizontal discretization leads to a different number of GWF cells between the delivery and return pipes of the U-shaped BHE (as shown in Fig. 7).

As shown in Fig. 7, for models with a minimum cell size of 0.5 cm, 12 cells are present between the inlet and outlet pipes cells, whereas, for the remaining models, these CLN nodes are placed into two adjacent GWF cells. The presence of multiple cells between the two pipes provides an accurate interpolation between adjacent cells, able to detect the temperature increase occurring in that specific portion of the domain. Thus, the CLN nodes that identify the return pipe are in contact with colder cells than those around the delivery pipe, exchanging heat with the GWF domain nearby. This progressively decreases the heat carrier fluid

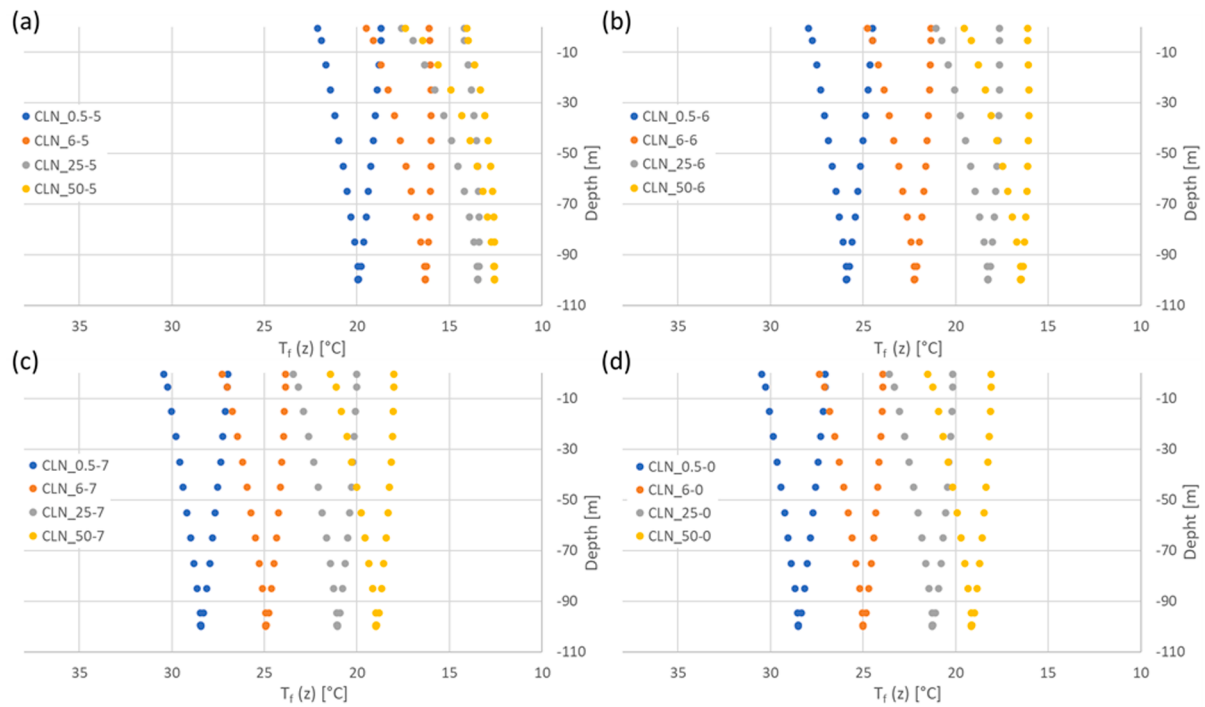


Fig. 6. Heat carrier fluid temperature as a function of depth after 10 days of constant heat rate injection for models “CLN_*-5” (a), 30 days for models “CLN_*-6” (b), 60 days for models “CLN_*-7” (c) and “CLN_*-0” (d).

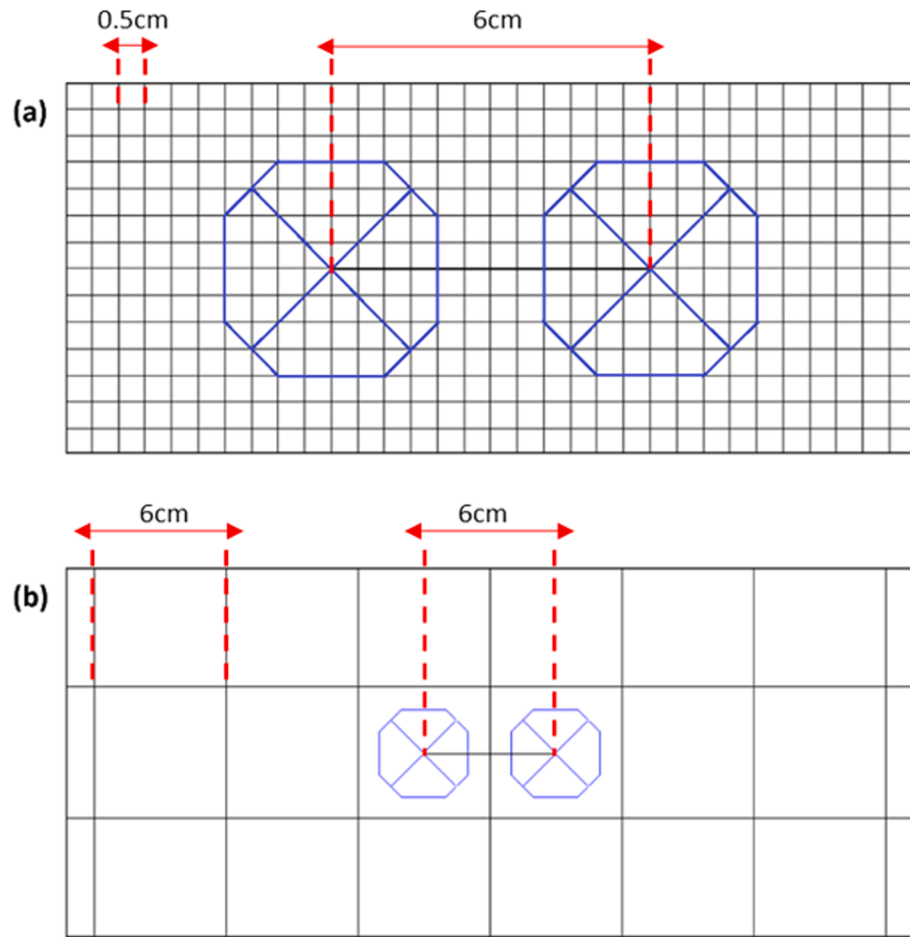


Fig. 7. Detail of the plan view of the modeling domain between the supply and return pipes into the “CLN_0.5-*” models (a) and into the “CLN_6-*” model (b).

temperature and provides a correct distribution of fluid temperature along the depth. On the other hand, when the U-pipe extreme cells are adjacent (Fig. 7b) the heat exchange occurs between a very warm cell (inlet) and a very cold one (outlet) hindering an accurate simulation of the temperature distribution among nodes inside the BHE. As expected, the behavior is more emphasized as the minimum cell size and the groundwater flow velocity increase.

3.2. Aquifer temperature: grid sensitivity analysis for different Darcy velocities

The horizontal thermal aquifer profile is reported in Fig. 8, where temperature values are extracted at difference distances downgradient from the BHE in correspondence of 11 observation points, shown in Fig. 4, at the last time step of each simulation. This allows to analyze the groundwater thermal perturbation around the BHE. The constant heat rate injection for each simulation is defined in Table 4 (q_{num}).

The graphs show that as groundwater flow increases (i.e. "CLN_*-5" and "CLN_*-6"), the thermal plume moves downstream more quickly, perturbing the aquifer even in the area farthest from the U-tube. Models with groundwater flow velocity equal to 10^{-7} and 0 m/s (i.e. "CLN_*-7" and "CLN_*-0") show higher temperatures around the BHE and a less extended thermal plume, which leads to the natural groundwater temperature in the first meters downstream.

The horizontal grid discretization exerts an influence on aquifer temperatures, which is greater in the first 3 m downstream and in models characterized by a higher groundwater velocity. In detail, models more affected by the spatial discretization are those with minimum cell size equal to 25 and 50 cm ("CLN_25-5", "CLN_25-6", "CLN_50-5" and "CLN_50-6"). When groundwater flow velocity decreases, the influence of the horizontal grid discretization is detectable only with models with a minimum cell size of 50 cm ("CLN_50-7" and "CLN_50-0").

Inside the GWF domain, the heat exchange computed between adjacent cells is strictly related to the resolution of the model grid, as discussed for the heat carrier fluid temperature results. When the

domain grid is highly refined, the heat exchange between adjacent nodes is more precise, thus maintaining higher temperatures around the BHE and simulating an accurate thermal plume regardless of the Darcy velocity implemented in the model. In contrast, in wider grids, nodes are placed at greater distances, so temperature values are averaged over larger cells. Therefore, these models are associated with globally lower aquifer temperatures near the BHE, especially for advection-dominated models.

3.3. Validation against analytical solution

To assess the robustness of the new numerical modeling approach, a comparison with analytical solutions is performed, such as discussed in literature. As already described in subsection 2.5, ILS and MLS analytical solutions are implemented to perform a comparison both with the purely conductive and the advective case, in terms of aquifer temperatures (Fig. 8) and equivalent exchanged heat rate (Table 5). The constant input heat rate value set in each analytical solution is the exchanged amount by the corresponding numerical model (shown in Table 4 as q_{num}). This choice allows to compare groundwater temperatures when numerical model and analytical solution have the exact same value of input heat rate. In Fig. 9 the aquifer temperature values are considered

Table 5

Results of the validation process in terms of q_{fit} and Δq achieved for the models implemented in MODFLOW-USG and the "MA" model.

	10^{-5} m/s		10^{-6} m/s		10^{-7} m/s		0	
	q_{fit} [W/ m]	Δq [%]						
CLN_0.5	39.5	0.3	39.2	0.1	39.2	0.4	39.3	0.7
CLN_6	39.0	-0.7	38.7	-1.3	39.2	0.3	39.4	0.7
CLN_25	30.2	-22.6	35.2	-10.4	38.7	-1.5	39.4	0.4
CLN_50	27.9	-27.4	31.9	-18.8	36.4	-7.4	37.5	-4.7
MA	36.4	-9.0	36.8	-8.0	39.5	-1.2	40.7	1.7

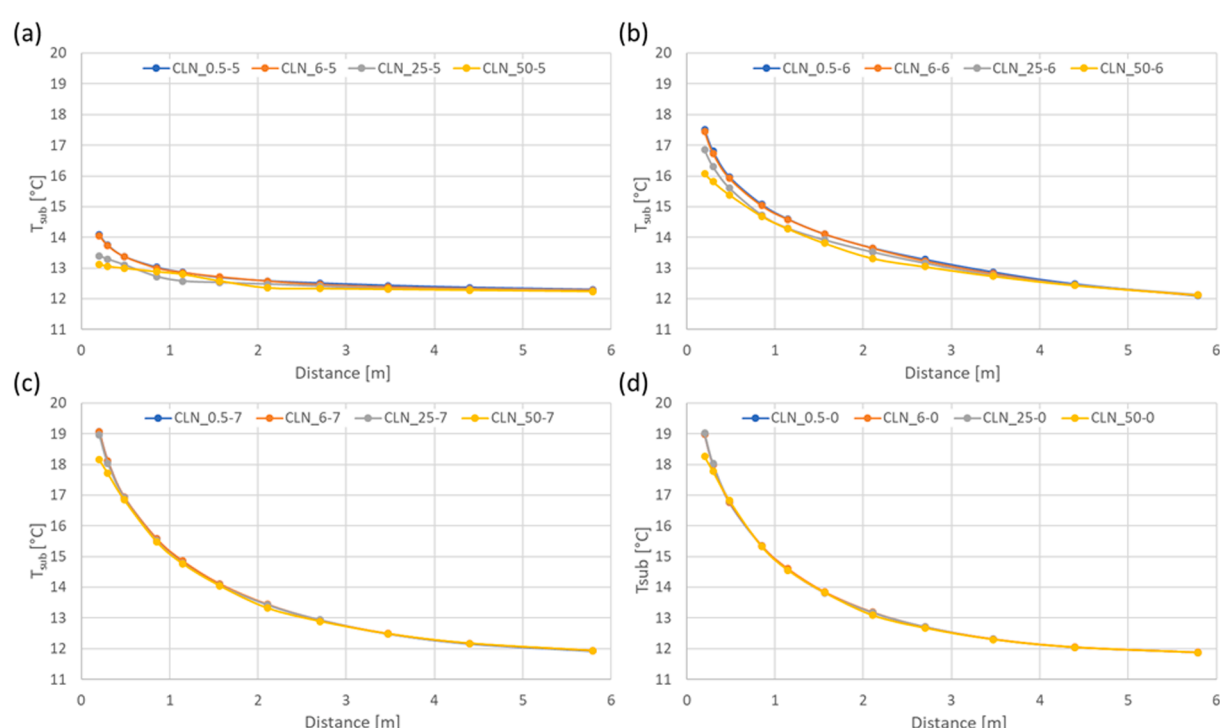


Fig. 8. Aquifer temperature downstream of the BHE at 35 m depth, after 10 days of constant heat injection for model "CLN_*-5" (a), 30 days for model "CLN_*-6" (b), 60 days for models "CLN_*-7" (c) and "CLN_*-0" (d), for each grid discretization.

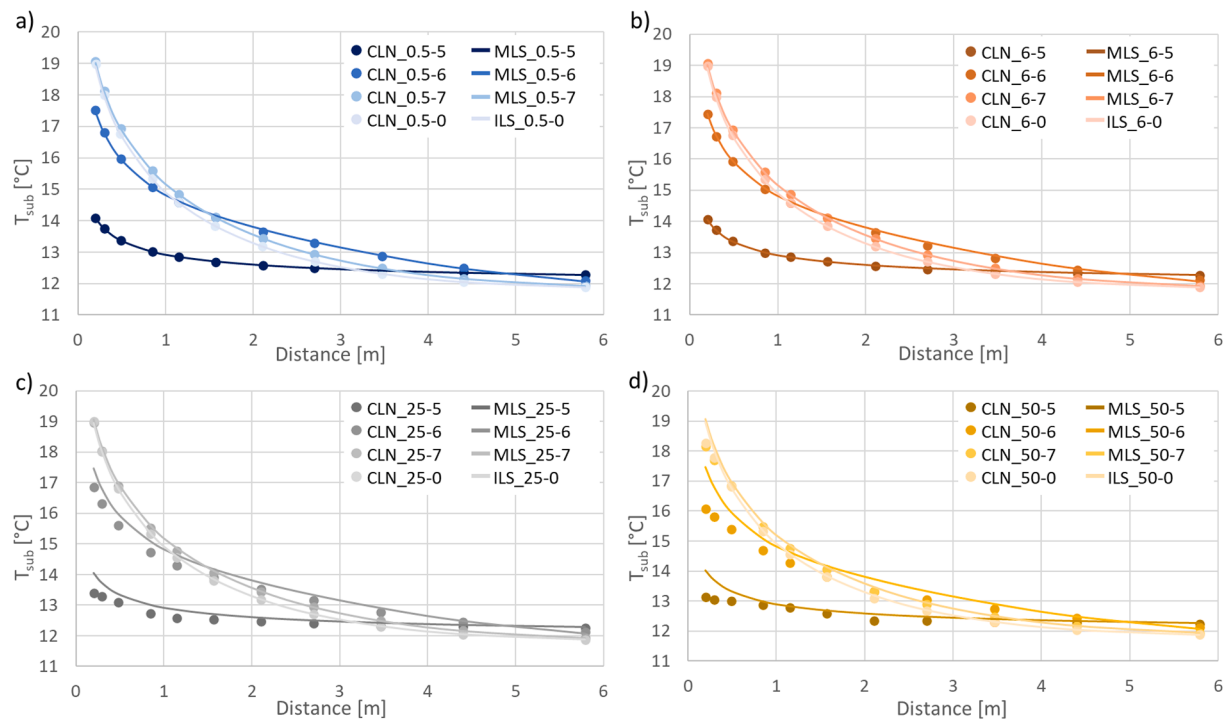


Fig. 9. Aquifer temperature downstream of the BHE according to the MLS and ILS models and to the MODFLOW-USG simulations running “CLN_0.5-*” (a), “CLN_6-*” (b), “CLN_25-*” (c) and “CLN_50-*” (d) models.

at the same domain points between numerical and analytical solution (from 20 cm to 6 m downgradient of the BHE), for different groundwater flows. The results are shown at the last time step of each simulation based on different groundwater flow velocities.

For models with a minimum cell size of 0.5 cm and 6 cm (Fig. 9a, b) a good agreement is achieved between the analytical and numerical temperature profiles for each groundwater flow velocity, with deviations lower than 0.2 °C in absolute value. In contrast, models with a minimum cell size of 25 cm and 50 cm (Fig. 9c, d) are associated with greater deviations. In particular, in Fig. 9c higher errors are achieved near the BHE for higher Darcy velocities (“CLN_25-5” and “CLN_25-6”); Fig. 8d shows larger deviations for all groundwater velocities, with greater errors associated with velocity of 10^{-5} and 10^{-6} m/s. The maximum deviation, equal to 1.4 °C, is registered for model “CLN_50-6”. These results are in accordance with those discussed in subsection 3.2: the main deviations between analytical and numerical results were found in “CLN_25-5”, “CLN_25-6” and “CLN_50-*” models, less accurate in the first 2 m downstream of the BHE because of the wider grid discretization. Table 5 shows the results of the validation process in terms of q_{fit} and index of accuracy Δq previously defined (eq. (2)).

As expected, “CLN_0.5-*” and “CLN_6-*” models accurately simulate the constant heat rate injection results, regardless of the groundwater flow value implemented, producing a maximum relative discrepancy between q_{num} and q_{fit} , in absolute terms, equal to 1.3 %. In energy terms, models with a minimum cell size equal to 0.5 cm and 6 cm show an excellent agreement with the analytical solution both in the purely conductive case and in the advective ones. On the other hand, “CLN_25-*” and “CLN_50-*” models show higher percentage errors for groundwater flow velocity equal to 10^{-5} and 10^{-6} m/s, with a maximum overestimation equal to 27.4 %. Therefore, for the same models, a better agreement with the analytical solution is highlighted when the transport is mainly conductive.

Furthermore, the results in Table 5 show that “CLN_0.5-*” and “CLN_6-*” models reach a better agreement with the analytical solution than “MA” model, for all the analyzed groundwater velocities. The improvement is more noteworthy for the high Darcy cases, namely 10^{-6}

and 10^{-5} m/s. Therefore, the new approach confirms and improves the results shown in (Angelotti et al., 2014a), although the simulation runtimes with the new techniques are shorter.

Although the validation process has shown errors below 5 % even for “CLN_25-7”, “CLN_25-0” and “CLN_50-0” models, the most suitable models for the TRT numerical simulation regardless of Darcy velocity, are the ones with a minimum cell size equal to 0.5 and 6 cm. Indeed, the use of minimum cell sizes ensures both to keep the heat rate constant over the time and to accurately simulate the heat exchange inside the aquifer and the U-pipe.

4. Conclusions

Over the past decade, progress achieved in numerical codes for simulating groundwater flow in porous media and related processes led to an increasing use of numerical models as alternative tools to analytical ones for Thermal Response Tests interpretation and typical BHE simulation.

Starting from the results discussed in (Antelmi et al., 2021), this study upgrades the MODFLOW-USG CLN package in order to improve its capability in simulating BHE, and mainly focusing on the possibility to implement a numerical TRT into the Control Volume Finite Difference. This has been achieved using a new approach based on CLN and DRT packages. To support the study, the proposed methodology is tested considering the detailed numerical model described in (Angelotti et al., 2014a) and well-known analytical models (ILS and MLS). In the present study 16 numerical models are implemented by combining four different Darcy velocities ranging from 0 to 10^{-5} m/s (representing a broad range of groundwater velocities in aquifers), and four minimum cell sizes in the horizontal grid discretization around the BHE, ranging from 0.5 to 50 cm. Quadtree refinement around the BHE, a special tool to refine grid available for MODFLOW-USG, is implemented to lighten the computational load. Each model implements a uniform, non-dispersive geologic medium with the same hydrogeologic and thermal properties defined in (Angelotti et al., 2014a), where a vertical BHE consisting of a single HDPE U-tube is implemented.

The results show that the new approach correctly simulates a constant heat rate operation, typical of a TRT procedure, maintaining constant the exchanged heat rate between the BHE and the surrounding aquifer over the time. For the more refined grid models, the average heat rate corresponding to the entire simulation deviates less than 2 % from the design heat rate imposed by the DRT package. Nevertheless, the implementation of coarse grids can lead to an underestimation of the heat carrier fluid mean temperature and, in the case of higher Darcy velocities, to an approximate heat exchange between the BHE and the aquifer. Moreover, coarser grids tend to distort the profile of the thermal plume that develops in the first 2–3 m downstream of the U-pipe. These results suggest that, for Darcy velocities higher than 10^{-6} m/s, the grid refinement around the borehole radius should be on the order of 6 cm to accurately investigate the thermal behavior of the aquifer in the first 3 m surrounding the BHE when conducting a TRT simulation. In case of lower velocities, a grid size of 25 cm can be adequate. In fact, the validation process proved that models with minimum cell sizes of 0.5 and 6 cm accurately simulate constant heat rate operation both in the purely conductive case and for groundwater velocities between 10^{-7} and 10^{-5} m/s, while less stringent refinements do not work optimally when the advective component is prevalent.

By way of contrast, when the aim of the study is mostly to assess the thermal impact in the aquifer beyond 3 m downstream of the BHE, a refinement in-between 25 and 50 cm is appropriate. Moreover, since the comparison with the results discussed in (Angelotti et al., 2014a) showed, for fine grids, lower errors for all the Darcy velocities analyzed, a TRT implementation or a BHE standard operation in MODFLOW-USG allows quicker, more efficient and accurate simulations than those performed in previous studies with MODFLOW and MT3DMS. Overall, the results achieved confirm the issues discussed in (Al-Khoury et al., 2005; Florides et al., 2012; Lamarche et al., 2010; Raymond et al., 2011; Signorelli et al., 2007): the implementation of a pseudo-3D model lightens considerably the computational load of numerical models representing GSHP systems, while guaranteeing a good accuracy in the results and providing the further possibility to implement the operation of many BHEs within the same modeling domain.

Future developments of this study will result in applying the proposed method to the simulation of real-world tests, either conventional or innovative (Enhanced TRT), to demonstrate its potential as a reliable TRT interpretation tool. As the installation of GSHP systems will become more frequent according to the decarbonization processes progressing in Europe, the results of the modeling approach presented will provide efficient and reliable support in optimizing the design of geothermal borefields.

Finally, having lightened the computational load and demonstrated the good accuracy of the results, from now on it will be possible to apply MODFLOW-USG to forecast the thermal impact of multiple geothermal plants at community/urban scale, where many BHEs are operating. As in the major European cities these energy systems are continuously growing, this will represent an important tool to identify potential overlapping of thermal plumes, allowing the regulatory authorities to manage this underground energy resource in a sustainable way, avoiding its over-exploitation over the foreseeable future.

CRediT authorship contribution statement

Sara Barbieri: Software, Validation, Investigation, Data curation, Writing – original draft, Visualization. **Matteo Antelmi:** Methodology, Validation, Investigation, Data curation, Writing – original draft, Supervision. **Sorab Panday:** Resources, Software, Writing – review & editing. **Martina Baratto:** Software, Investigation, Data curation, Writing – original draft. **Adriana Angelotti:** Methodology, Writing – review & editing. **Luca Alberti:** Methodology, Writing – review & editing, Supervision, Project administration.

Declaration of Competing Interest

The authors declare that they have no known competing financial interests or personal relationships that could have appeared to influence the work reported in this paper.

Data availability

Data will be made available on request.

References

- Alberti, L., Angelotti, A., Antelmi, M., La Licata, I., 2016. Borehole Heat Exchangers in aquifers: Simulation of the grout material impact. *Rend. Online Soc. Geol. Ital.* 41 <https://doi.org/10.3301/ROL.2016.145>.
- Alberti, L., Angelotti, A., Antelmi, M., La Licata, I., 2017. A numerical study on the impact of grouting material on borehole heat exchangers performance in aquifers. *Energies* 10. <https://doi.org/10.3390/en10050703>.
- Al-Khoury, R., Bonnier, P.G., Brinkgreve, R.B.J., 2005. Efficient finite element formulation for geothermal heating systems. Part I: steady state. *Int. J. Numer. Methods Eng.* 63, 988–1013. <https://doi.org/10.1002/NME.1313>.
- Angelotti, A., Alberti, L., La Licata, I., Antelmi, M., 2014a. Energy performance and thermal impact of a Borehole Heat Exchanger in a sandy aquifer: Influence of the groundwater velocity. *Energy Convers. Manag.* 77, 700–708. <https://doi.org/10.1016/j.enconman.2013.10.018>.
- Angelotti, A., Alberti, L., La Licata, I., Antelmi, M., 2014b. Borehole heat exchangers: Heat transfer simulation in the presence of a groundwater flow. *J. Phys. Conf. Ser.* 501 <https://doi.org/10.1088/1742-6596/501/1/012033>.
- Antelmi, M., Alberti, L., Angelotti, A., Curnis, S., Zille, A., Colombo, L., 2020a. Thermal and hydrogeological aquifers characterization by coupling depth-resolved thermal response test with moving line source analysis. *Energy Convers. Manag.* 225, 113400 <https://doi.org/10.1016/j.enconman.2020.113400>.
- Antelmi, M., Renoldi, F., Alberti, L., 2020b. Analytical and numerical methods for a preliminary assessment of the remediation time of pump and treat systems. *Water (Switzerland)* 12. <https://doi.org/10.3390/w12102850>.
- Antelmi, M., Alberti, L., Barbieri, S., Panday, S., 2021. Simulation of thermal perturbation in groundwater caused by Borehole Heat Exchangers using an adapted CLN package of MODFLOW-USG. *J. Hydrol.* 596 <https://doi.org/10.1016/j.jhydrol.2021.126106>.
- Attard, G., Bayer, P., Rossier, Y., Blum, P., Eisenlohr, L., 2020. A novel concept for managing thermal interference between geothermal systems in cities. *Renew. Energy* 145, 914–924. <https://doi.org/10.1016/j.renene.2019.06.095>.
- Bandos, T.V., Montero, A., Fernández, E., Santander, J.L.G., Isidro, J.M., Pérez, J., de Córdoba, P.J.F., Urchueguía, J.F., 2009. Finite line-source model for borehole heat exchangers: effect of vertical temperature variations. *Geothermics* 38, 263–270. <https://doi.org/10.1016/j.geothermics.2009.01.003>.
- Banks, D., 2012. From Fourier to Darcy, from Carslaw to Theis: the analogies between the subsurface behaviour of water and heat. *Acque Sotter. – Ital. J. Groundw.* 1, 009–018. <https://doi.org/10.7343/AS-013-12-0025>.
- Beier, R.A., 2021. Analysis of thermal response tests on boreholes with controlled inlet temperature versus controlled heat input rate. *Geothermics* 94, 102099. <https://doi.org/10.1016/j.geothermics.2021.102099>.
- Berberich, H., Fisch, N., Hahne, E., 1994. Field experiments with a single duct in water saturated claystone. *Int. Conf. Therm. Energy Storage, Calorstock* 2, 341–348.
- Blasi, A., Menichetti, M., 2012. Thermal conductivity distributed from a Thermal Response Test (TRT) in a borehole heat exchanger (BHE). *Ital. J. Groundw.* 41–48 <https://doi.org/10.7343/AS-010-12-0027>.
- Bozzoli, F., Pagliarini, G., Rainieri, S., Schiavi, L., 2011. Estimation of soil and grout thermal properties through a TSPEP (two-step parameter estimation procedure) applied to TRT (thermal response test) data. *Energy* 36, 839–846. <https://doi.org/10.1016/J.ENERGY.2010.12.031>.
- Brunetti, G., Saito, H., Saito, T., Šimůnek, J., 2017. A computationally efficient pseudo-3D model for the numerical analysis of borehole heat exchangers. *Appl. Energy* 208, 1113–1127. <https://doi.org/10.1016/J.APENERGY.2017.09.042>.
- Carlslaw, H., Jaeger, J.C., 1959. *Heat Conduction in Solids*. Oxford University Press.
- Casasso, A., Piga, B., Sethi, R., Prestor, J., Pestotnik, S., Bottig, M., Goetzl, G., Zambelli, P., D'Alonzo, V., Vaccaro, R., Capodaglio, P., Olmedo, M., Baietto, A., Maragna, C., Böttcher, F., eder, K.Z., 2017. The GRETA project: the contribution of near-surface geothermal energy for the energetic self-sufficiency of Alpine regions. *Acque Sotter. – Ital. J. Groundw.* 6, 23–33. <https://doi.org/10.7343/as-2017-265>.
- Casasso, A., Sethi, R., 2014. Efficiency of closed loop geothermal heat pumps: a sensitivity analysis. *Renew. Energy* 62, 737–746. <https://doi.org/10.1016/j.renene.2013.08.019>.
- Chae, H., Nagano, K., Katsura, T., Sakata, Y., Serageldin, A.A., 2022. Life cycle cost analysis of ground source heat pump system based on multilayer thermal response test. *Energy Build.* 261, 111427 <https://doi.org/10.1016/j.enbuild.2021.111427>.
- European Commission, 2021. Global status report for Buildings and construction.
- Dalla Santa, G., Pasquier, P., Schenato, L., Galgaro, A., 2022. Repeated ETRTs in a complex stratified geological setting: high-resolution thermal conductivity identification by multiple linear regression. *J. Geotech. Geoenvir. Eng.* 148, 1–15. [https://doi.org/10.1061/\(asce\)gt.1943-5606.0002724](https://doi.org/10.1061/(asce)gt.1943-5606.0002724).

- Diao, N., Li, Q., Fang, Z., 2004. Heat transfer in ground heat exchangers with groundwater advection. *Int. J. Therm. Sci.* 43, 1203–1211. <https://doi.org/10.1016/j.ijthermalsci.2004.04.009>.
- Eskilson, P., 1987. Thermal Analysis of Heat Extraction Boreholes. Response 222.
- Farabi-Asl, H., Chapman, A., Itaoka, K., Noorollahi, Y., 2019. Ground source heat pump status and supportive energy policies in Japan. *Energy Procedia* 158, 3614–3619. <https://doi.org/10.1016/j.egypro.2019.01.902>.
- Florides, G.A., Christodoulides, P., Pouloupatis, P., 2012. An analysis of heat flow through a borehole heat exchanger validated model. *Appl. Energy* 92, 523–533. <https://doi.org/10.1016/J.APENERGY.2011.11.064>.
- Fujii, H., Itoi, R., Fujii, J., Uchida, Y., 2005. Optimizing the design of large-scale ground-coupled heat pump systems using groundwater and heat transport modeling. *Geothermics* 34, 347–364. <https://doi.org/10.1016/j.geothermics.2005.04.001>.
- Galgaro, A., Dalla Santa, G., Zarrella, A., 2021. First Italian TRT database and significance of the geological setting evaluation in borehole heat exchanger sizing. *Geothermics* 94, 102098. <https://doi.org/10.1016/j.geothermics.2021.102098>.
- Gehlin, S., 2002. Thermal Response Test. Method Development and Evaluation. Luleå Univ. Technol. 191.
- Giordano, N., Lamarche, L., Raymond, J., 2021. Evaluation of subsurface heat capacity through oscillatory thermal response tests[†]. *Energies* 14. <https://doi.org/10.3390/en14185791>.
- Jodeiri, A.M., Goldsworthy, M.J., Buffa, S., Cozzini, M., 2022. Role of sustainable heat sources in transition towards fourth generation district heating – a review. *Renew. Sustain. Energy Rev.* 158, 112156 <https://doi.org/10.1016/j.rser.2022.112156>.
- Lamarche, L., Kajl, S., Beauchamp, B., 2010. A review of methods to evaluate borehole thermal resistances in geothermal heat-pump systems. *Geothermics* 39, 187–200. <https://doi.org/10.1016/J.GEOTHERMICS.2010.03.003>.
- Li, R., Ooka, R., Shukuya, M., 2014. Theoretical analysis on ground source heat pump and air source heat pump systems by the concepts of cool and warm exergy. *Energy Build.* 75, 447–455. <https://doi.org/10.1016/j.enbuild.2014.02.019>.
- Regione Lombardia, 2010. Interventi normativi per l'attuazione della programmazione regionale e di modifica e integrazione di disposizioni legislative – Collegato ordinamentale 2011.
- Lyu, W., Li, X., Yan, S., Jiang, S., 2020. Utilizing shallow geothermal energy to develop an energy efficient HVAC system. *Renew. Energy* 147, 672–682. <https://doi.org/10.1016/j.renene.2019.09.032>.
- Man, Y., Yang, H., Diao, N., Liu, J., Fang, Z., 2010. A new model and analytical solutions for borehole and pile ground heat exchangers. *Int. J. Heat Mass Transf.* 53, 2593–2601. <https://doi.org/10.1016/j.ijheatmasstransfer.2010.03.001>.
- Marcotte, D., Pasquier, P., 2008. On the estimation of thermal resistance in borehole thermal conductivity test. *Renew. Energy* 33, 2407–2415. <https://doi.org/10.1016/J.RENENE.2008.01.021>.
- Molina-Giraldo, N., Bayer, P., Blum, P., 2011. Evaluating the influence of thermal dispersion on temperature plumes from geothermal systems using analytical solutions. *Int. J. Therm. Sci.* 50, 1223–1231. <https://doi.org/10.1016/j.ijthermalsci.2011.02.004>.
- Naldi, C., Zanchini, E., 2019. Full-time-scale fluid-to-ground thermal response of a borefield with uniform fluid temperature. *Energies* 12. <https://doi.org/10.3390/en12193750>.
- Nieto, I.M., Blázquez, C.S., Martín, A.F., González-Aguilera, D., 2020. Analysis of the influence of reducing the duration of a thermal response test in a water-filled geothermal borehole located in Spain. *Energies* 13. <https://doi.org/10.3390/en13246693>.
- Pambou, C.H.K., Raymond, J., Miranda, M.M., Giordano, N., 2022. Estimation of In-Situ Heat Capacity and Thermal Diffusivity from Undisturbed Ground Temperature Profile Measured in Ground Heat Exchangers. 10.20944/preprints202203.0173.v1.
- Panday, S., Langevin, C.D., Niswonger, R.G., Ibaraki, M., Hughes, J.D., 2013. MODFLOW – USG Version 1: an unstructured grid version of MODFLOW for simulating groundwater flow and tightly coupled processes using a control volume finite-difference formulation. *U.S. Geol. Surv.* 66.
- Panday, S., 2020. USG-Transport Version 1.5.0: The Block-Centered Transport (BCT) Process for MODFLOW-USG.
- Pasquier, P., Lamarche, L., 2022. Analytic expressions for the moving infinite line source model. *SSRN Electron. J.* 103, 102413 <https://doi.org/10.2139/ssrn.4011490>.
- Raymond, J., Therrien, R., Gosselin, L., Lefebvre, R., 2011. Numerical analysis of thermal response tests with a groundwater flow and heat transfer model. *Renew. Energy* 36, 315–324. <https://doi.org/10.1016/J.RENENE.2010.06.044>.
- Sakellaris, D., Lundqvist, P., 2003. Energy analysis of a low-temperature heat pump heating system in a single-family house. *Int. J. Energy Res.* 28, 1–12. <https://doi.org/10.1002/er.947>.
- Shonher, J.A., Beck, J.V., 1999. Determining effective soil formation thermal properties from field data using a parameter estimation technique. *ASHRAE Trans.* 105.
- Signorelli, S., Bassetti, S., Pahud, D., Kohl, T., 2007. Numerical evaluation of thermal response tests. *Geothermics* 36, 141–166. <https://doi.org/10.1016/J.GEOTHERMICS.2006.10.006>.
- Šimůnek, J., Genuchten, M.T., Šejna, M., 2016. Recent developments and applications of the HYDRUS computer software packages. *Vadose Zo. J.* 15, 1–25. <https://doi.org/10.2136/vzj2016.04.0033>.
- Spitzer, J.D., Gehlin, S.E.A., 2015. Thermal response testing for ground source heat pump systems—an historical review. *Renew. Sustain. Energy Rev.* 50, 1125–1137. <https://doi.org/10.1016/j.rser.2015.05.061>.
- Sutton, M.G., Nutter, D.W., Couvillion, R.J., 2003. A ground resistance for vertical bore heat exchangers with groundwater flow. *J. Energy Resour. Technol.* 125, 183–189. <https://doi.org/10.1115/1.1591203>.
- Wagner, V., Blum, P., Kübert, M., Bayer, P., 2013. Analytical approach to groundwater-influenced thermal response tests of grouted borehole heat exchangers. *Geothermics* 46, 22–31. <https://doi.org/10.1016/j.geothermics.2012.10.005>.
- Wagner, R., Clauer, C., 2005. Evaluating thermal response tests using parameter estimation for thermal conductivity and thermal capacity. *J. Geophys. Eng.* 2, 349–356. <https://doi.org/10.1088/1742-2132/2/4/S08>.
- Zeng, H.Y., Diao, N.R., Fang, Z.H., 2002. A finite line-source model for boreholes in geothermal heat exchangers. *Heat Transf. Res.* 31.
- Zhang, C., Guo, Z., Liu, Y., Cong, X., Peng, D., 2014. A review on thermal response test of ground-coupled heat pump systems. *Renew. Sustain. Energy Rev.* 40, 851–867. <https://doi.org/10.1016/j.rser.2014.08.018>.
- Zhang, C., Lu, J., Wang, X., Xu, H., Sun, S., 2022. Effect of geological stratification on estimated accuracy of ground thermal parameters in thermal response test. *Renew. Energy* 186, 585–595. <https://doi.org/10.1016/j.renene.2022.01.024>.
- Zong, Y., Valocchi, A.J., Lin, Y.F.F., 2021. Coupling a borehole thermal model and MT3DMS to simulate dynamic ground source heat pump efficiency. *Groundwater* 1–8. <https://doi.org/10.1111/gwat.13159>.